Electronic Supplementary Material (ESI) for Journal of Materials Chemistry A.
This journal is © The Royal Society of Chemistry 2019

Supporting material

Exploring the catalytic performance of a series of bimetallic MIL-100(Fe, Ni) MOFs

Mónica Giménez-Marqués,*[a,b] Andrea Santiago-Portillo,[c] Sergio Navalón,[c] Mercedes Álvaro,[c] Valérie Briois,[d] Farid Nouar,[a] Hermenegildo Garcia,*[c] Christian Serre.*[a]

[a] Institut des Matériaux Poreux de Paris, UMR 8004 CNRS, École Normale Supérieure, École Supérieure de Physique et de Chimie Industrielles de la ville de Paris, PSL University, 75005 Paris, France. [b] Instituto de Ciencia Molecular, Universidad de Valencia, Catedrático José Beltrán 2, 46980 Paterna, Spain. [c] Departamento de química e Instituto de Tecnología Química (ITQ-CSIC-Universitat Politècnica de València, C/Camino de Vera, s/n, 46022, Valencia, Spain). [d] Synchrotron SOLEIL-UR1, 91192, Gif-Sur-Yvette, France

Content

Thermogravimetric analyses

Thermogravimetric analyses were performed by a PerkinElmer STA 6000 apparatus. The measurements were conducted under O_2 with a heating rate of 5 °C.min^{-1}. All solids revealed comparable thermal stability up to 300 °C whereas weigh losses of the mixed-metal MOFs are in good agreement with the expected range: about 66% ligand loss for MIL-100(Fe, Ni) **1-3** (63% and 69% calc. for the Fe_3O and Fe_2NiO ratio, respectively).

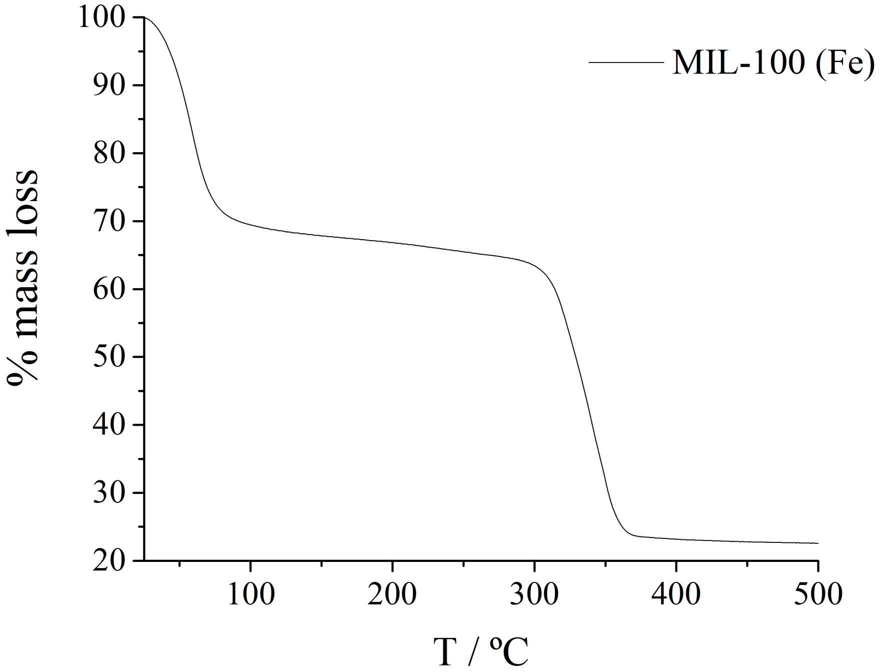

Figure S1. Thermogravimetric analysis of MIL-100(Fe).

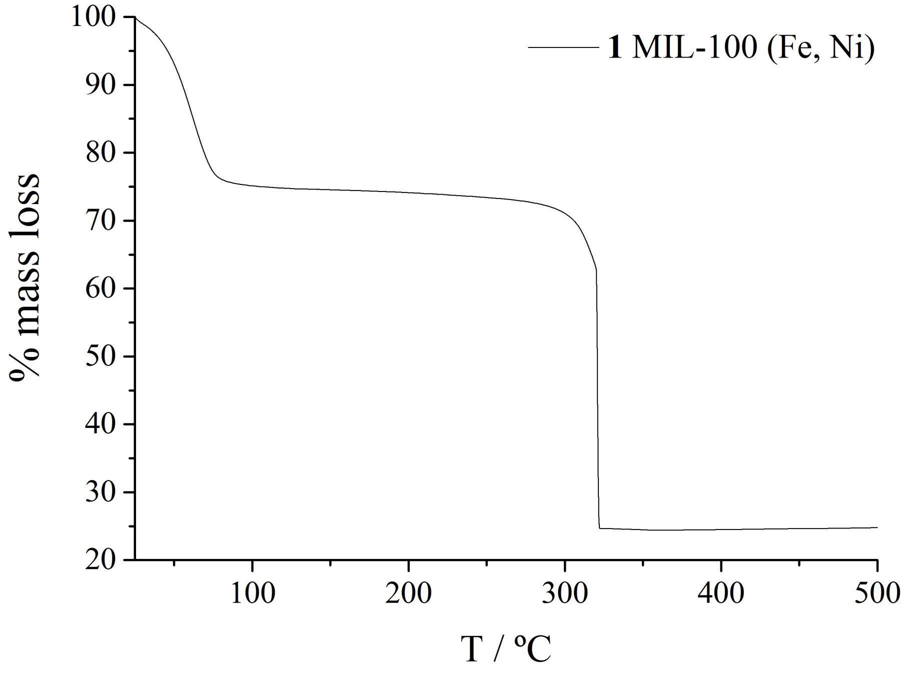

Figure S2. Thermogravimetric analysis of MIL-100(Fe, Ni) **1**.

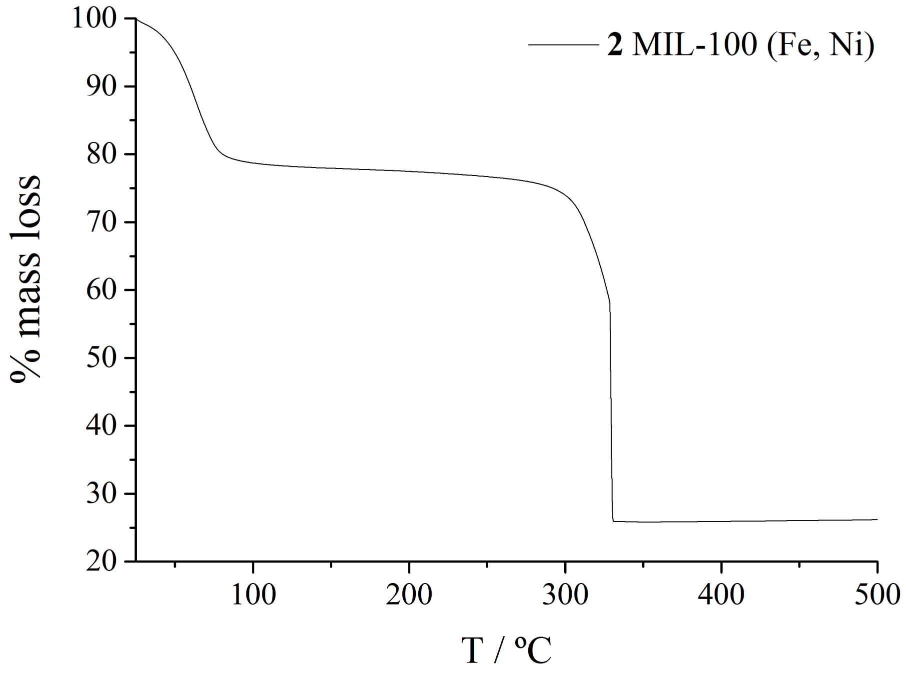

Figure S3. Thermogravimetric analysis of MIL-100(Fe, Ni) **2**.

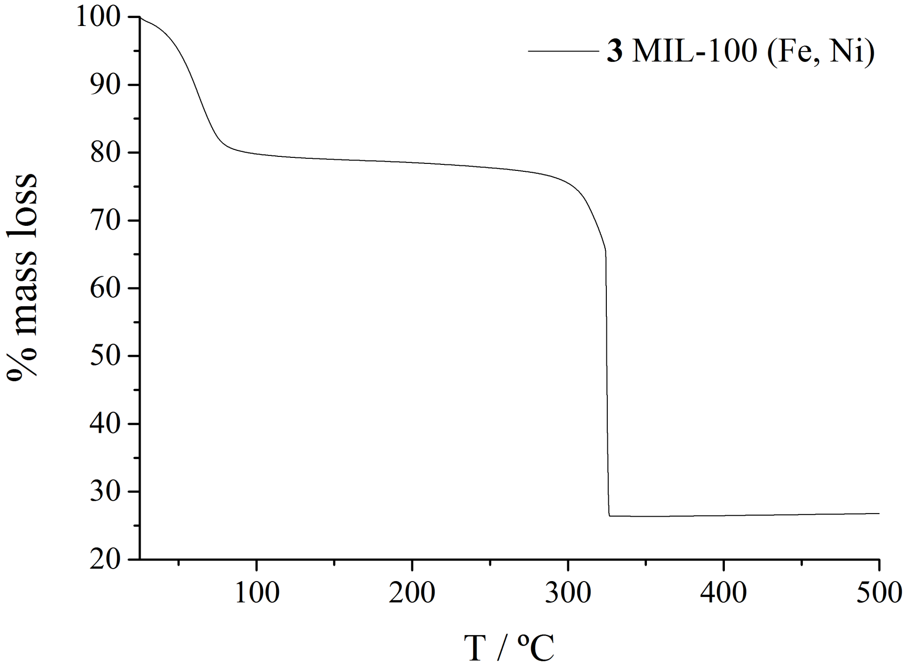

Figure S4. Thermogravimetric analysis of MIL-100(Fe, Ni) **3**.

IR spectroscopy

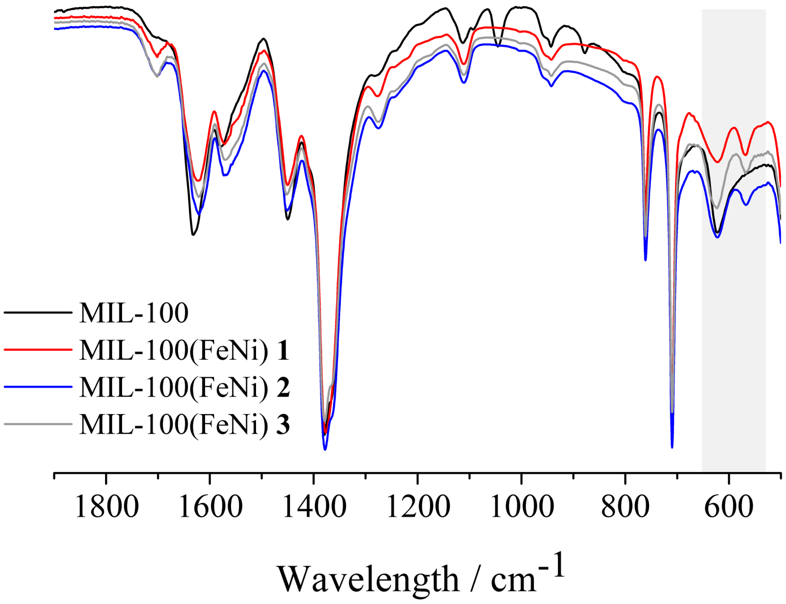

Figure S5. FT-IR spectra of MIL-100(Fe) (black) and MIL-100(Fe, Ni) **1-3** (red, blue and grey, respectively). All materials exhibit the characteristic asymmetric and symmetric stretching bands of the carboxylate anions respectively at 1630-1576 cm^{-1} and 1450-1382 cm^{-1}. The metal–oxygen bands of the $M_3(\mu_3\text{-}O)$ group is identified at 624 cm^{-1} in MIL-100(Fe) corresponding to the Fe_3O trimeric unit, whereas a new band appears at 569 cm^{-1} in **1-3** for the Fe_2NiO unit (see highlighted grey area).

Stability tests

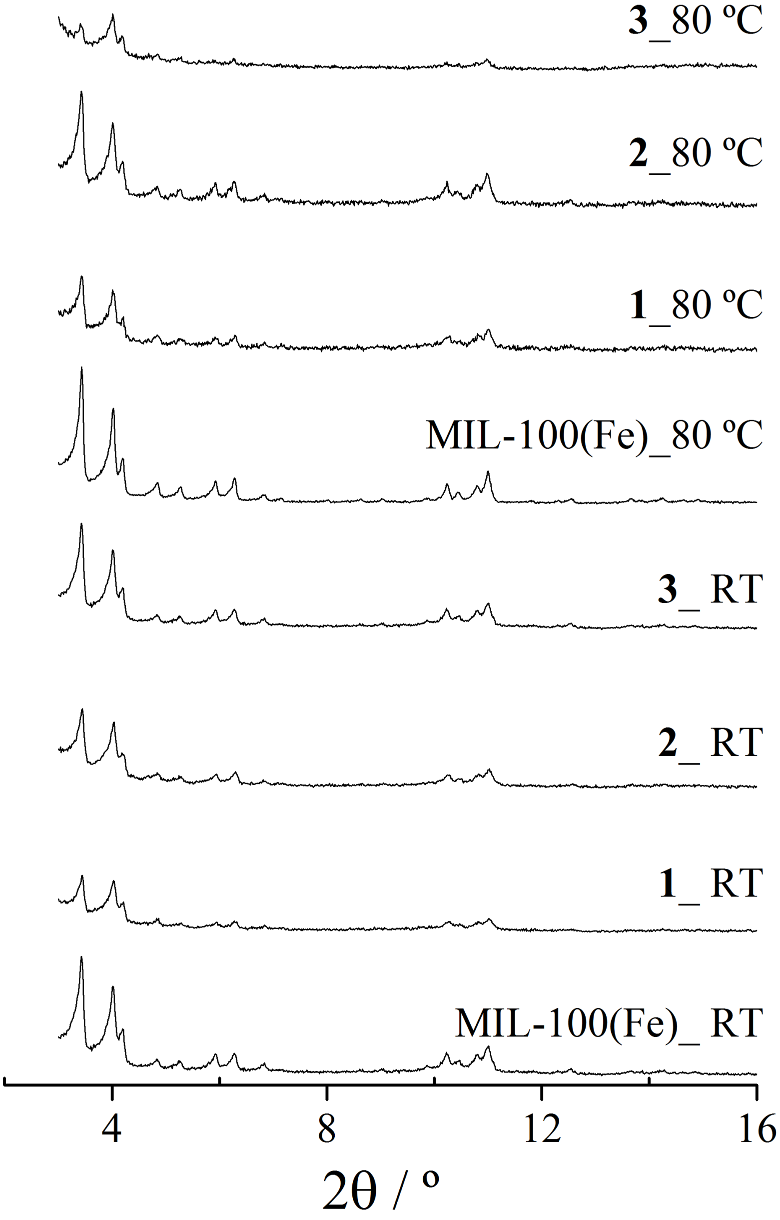

Figure S6. Powder X-ray diffraction patterns of mixed-metal MIL-100(Fe, Ni) **1-3** materials as compared with bare MIL-100(Fe) material after 24 h of stirring in water at room temperature (RT) and at 80 ºC.

Gas sorption studies

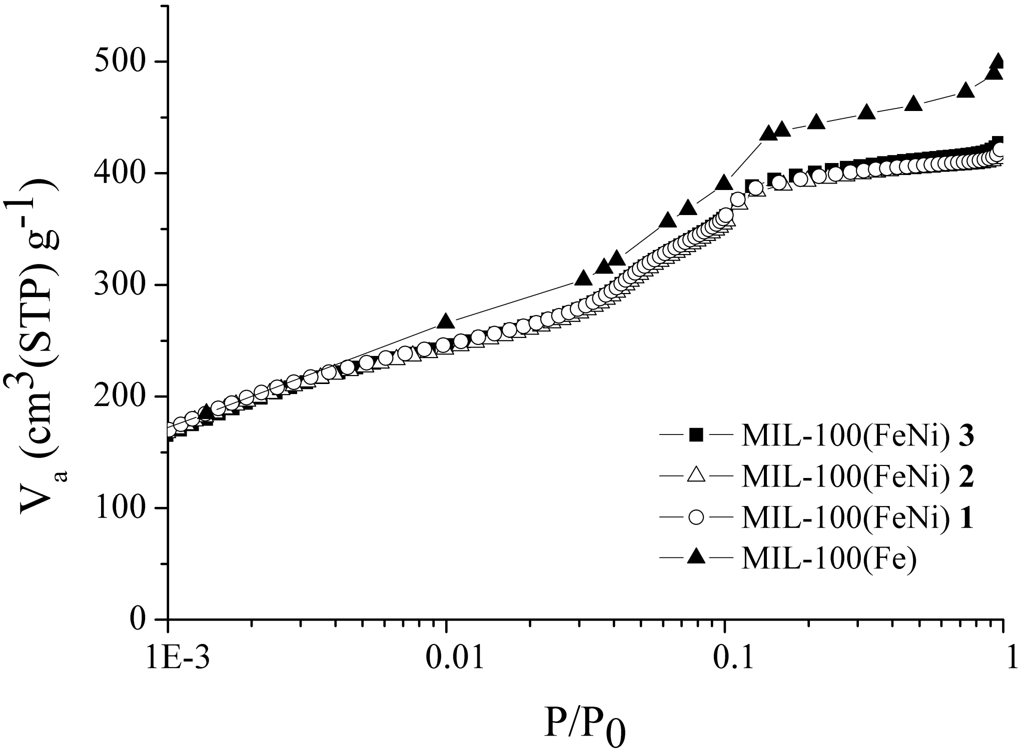

Figure S7. N_2 sorption isotherms for MIL-100(Fe) and MIL-100(Fe, Ni) **1-3** materials. Logarithmic scale of pressure range.

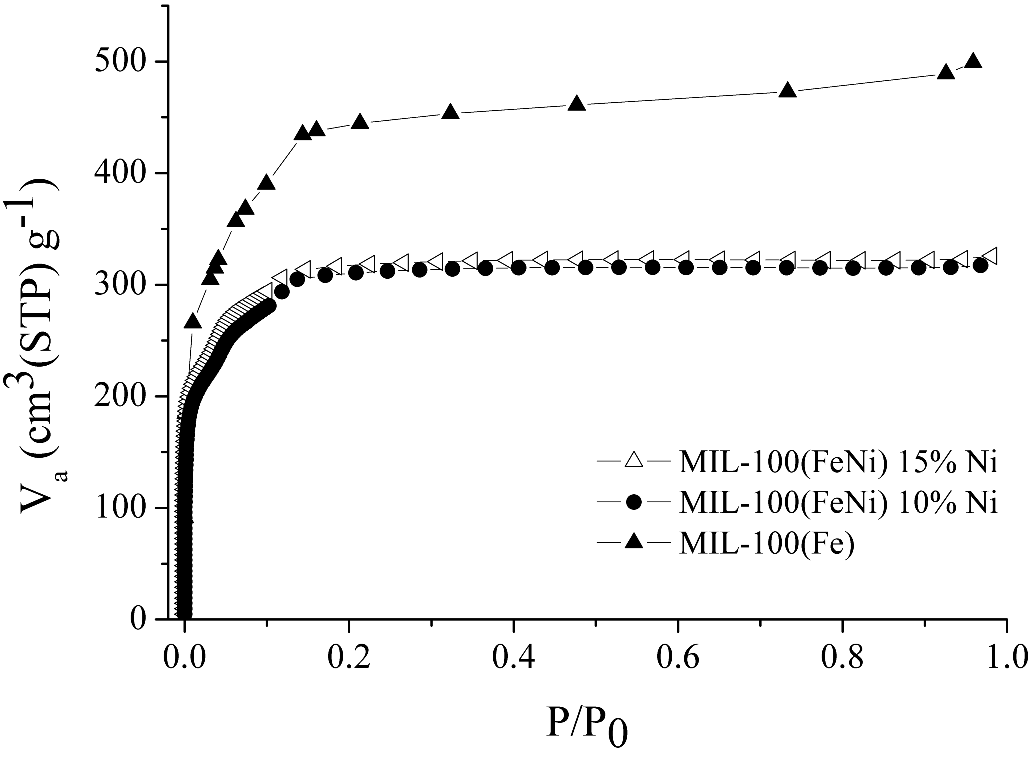

Figure S8. N_2 sorption isotherms for MIL-100(Fe, Ni) materials bearing 10 and 15 % of metal substitution.

SEM and EDX analysis

Iron/Nickel ratio was evaluated using a Jeol JSM-7001F microscope using gold coated samples equipped with an energy-dispersive X-ray (EDX) spectrometer with a X-Max SDD (Silicon Drift Detector) by Oxford. Some of the data was taken using a Jeol JSM-5800LV Scanning Microscope equipped with an integrated EDX system.

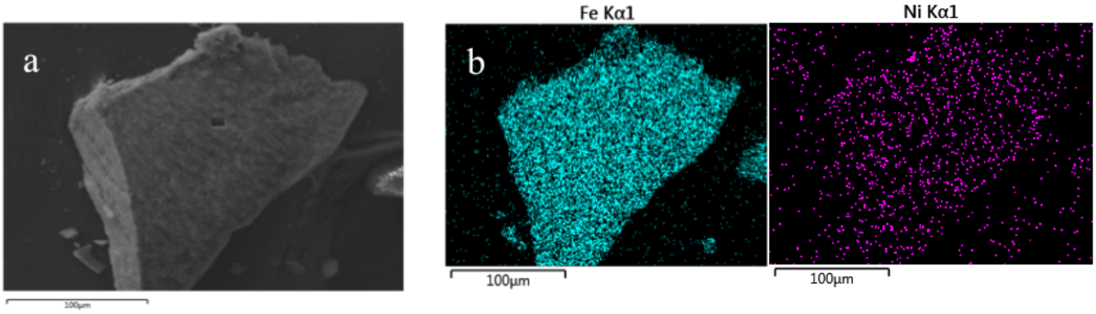

Figure S9. (a) SEM image and (b) energy dispersive X-ray spectroscopy (EDS) elemental mapping images of the MIL-100(Fe, Ni) **3**. Fe and Ni atoms appear as blue and purple colours, respectively. The regular distribution of Ni cations observed in the catalyst indicates the absence of undesired agglomerates or nanoparticles of Ni.

EXAFS studies

Local order and electronic structure characterizations at the Fe and Ni K edges were carried out at the ROCK beamline (SOLEIL, Gif-sur-Yvette) using the Si(111) channel-cut quick-EXAFS monochromator with an oscillation frequency of 2Hz. Higher harmonics were rejected by using two mirrors coated with B_4C at a grazing incidence of 2.8 mrad at both edges.

Pure MIL-100(Fe) and heterometallic MIL-100(Fe, Ni) **1-3** materials were prepared as pellets diluted with boron nitride. Measurements were carried out at Room Temperature in transmission mode. The Fe K edge EXAFS signal was extracted from a merge of 2500 spectra, each collected in 250 ms whereas Ni K edge signals were extracted from a merge of 3600 and 6700 spectra respectively for MIL-100(Fe, Ni) **1-3** materials, each spectrum collected in 250 ms.

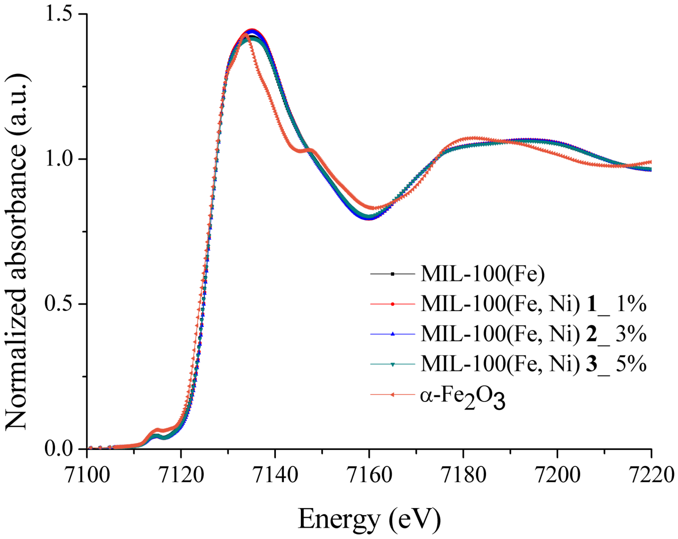

Figure S10. Fe Kedge XANES spectra for MIL-100(Fe) and MIL-100(Fe, Ni) **1-3** samples as compared to reference hematite sample.

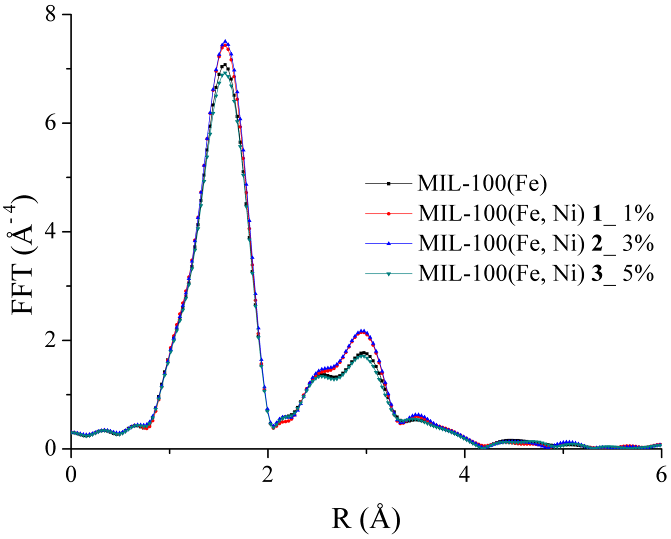

Figure S11. Fourier transforms of the Fe Kedge EXAFS spectra for MIL-100(Fe) and MIL-100(Fe, Ni) **1-3** samples.

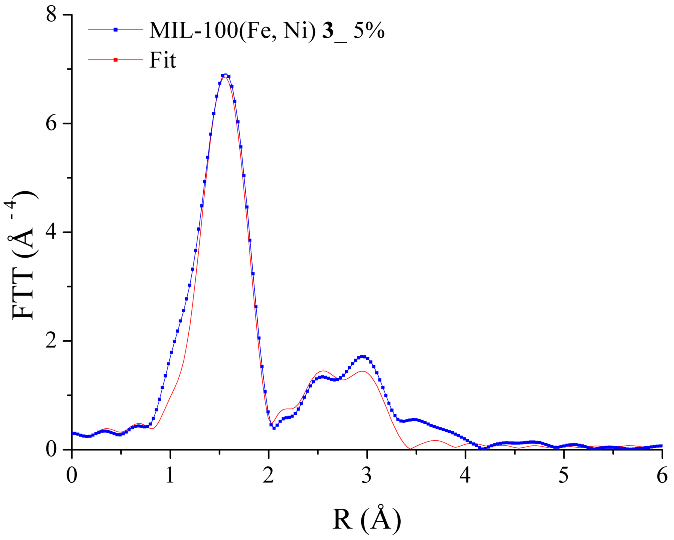

Figure S12. Simulation in R space of the Fourier transform of the Fe Kedge EXAFS spectrum for MIL-100(Fe, Ni) **3** sample.

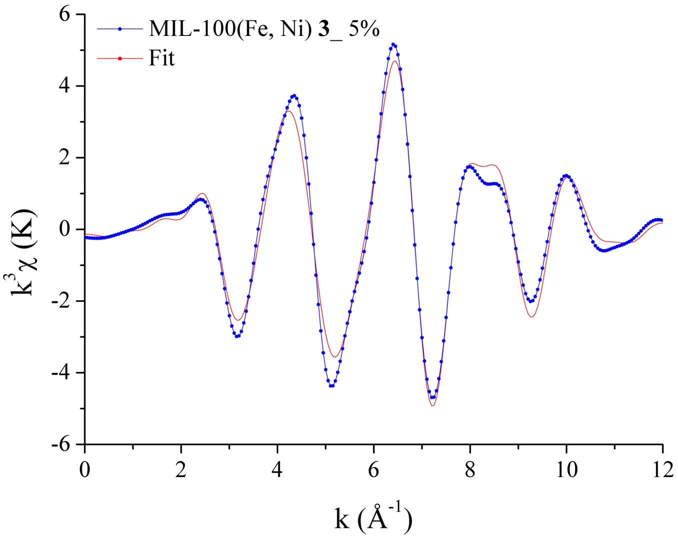

Figure S13. Fe Kedge spectra simulation in k space of the back-Fourier transform of the Fe K edge EXAFS spectrum for MIL-100(Fe, Ni) **3** sample.

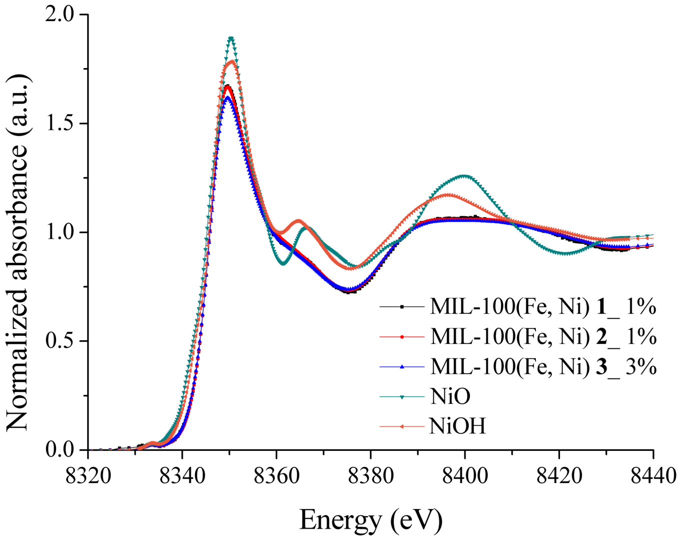

Figure S14. Ni Kedge XANES spectra for MIL-100(Fe, Ni) **1-3** samples as compared to reference NiO and NiOH samples.

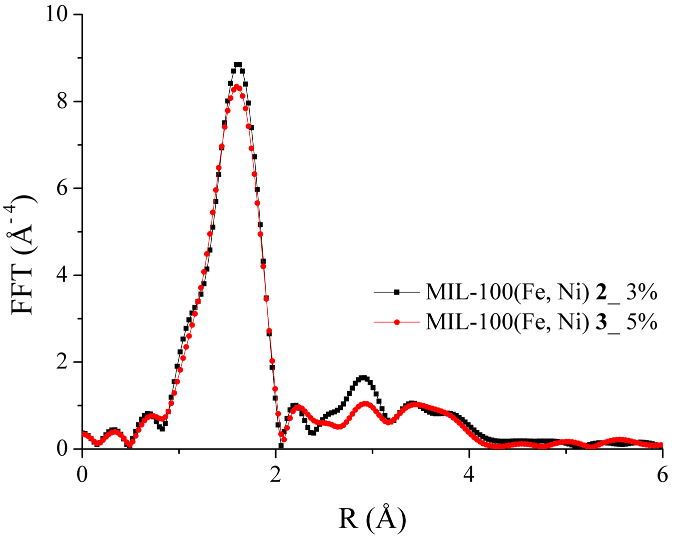

Figure S15. Fourier transforms of the Ni Kedge EXAFS spectra for MIL-100(Fe, Ni) **2** and MIL-100(Fe, Ni) **3** samples.

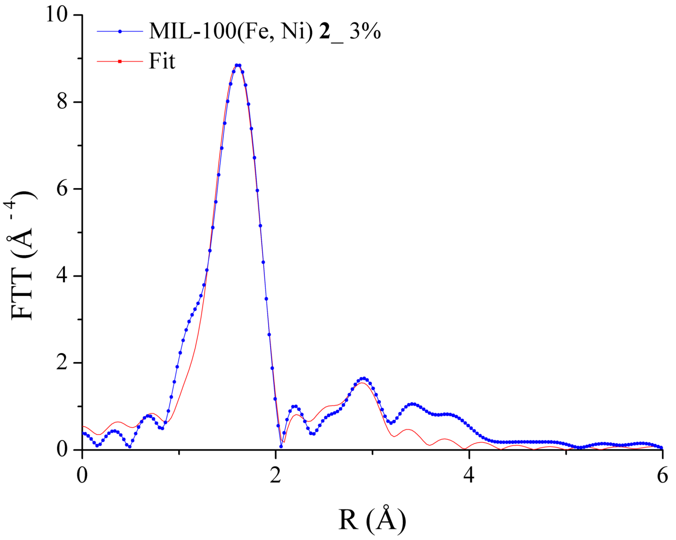

Figure S16. Simulation in R space of the Fourier transform of the Ni Kedge EXAFS spectrum for MIL-100(Fe, Ni) **2** sample.

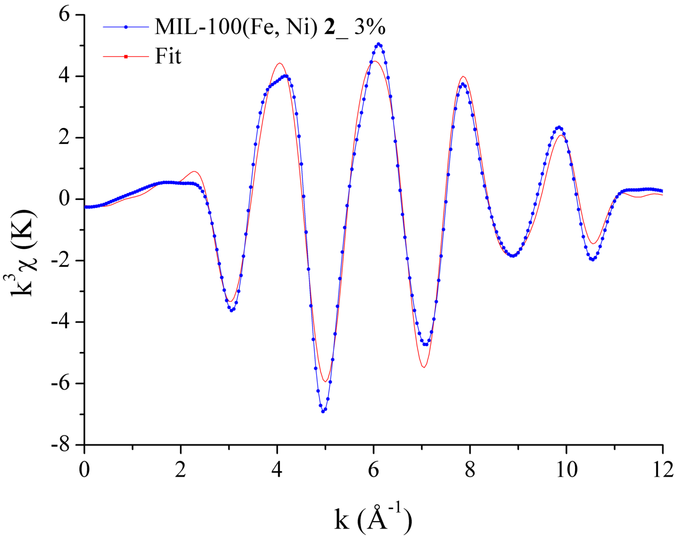

Figure S17. Simulation in k space of the back-Fourier transform of the Ni K edge EXAFS spectrum for MIL-100(Fe, Ni) **2** sample.

Table S1. Structural parameters determined by least square fitting of the EXAFS spectra recorded at the Ni K edge and Fe K edge Fit for sample MIL-100(Fe, Ni) **2** and **3**.

		Fixed values	**R (Å)**	**σ^2(Å^2) .10^{-3}**	**R_f χ^2_{red}**
Ni K edge		3 O	2.04 ± 0.02	5.5 ± 2.8	
S_0^2 = 1.23		3 O	2.10 ± 0.02	10.3 ± 4.6	
enot= 8345.6 ± 3.4 eV	MIL-100(Fe, Ni) **2** (3%)	4 C	3.05 ± 0.05	19.6 ± 12.9	0.9 %
Δk = 3.3 – 10 Å^{-1}		0.86 Fe	3.29 ± 0.04	1.4 ± 5.3	1118
ΔR = 1-4.2 Å		1.14 Fe	3.47 ± 0.05	5.8 ± 8.4	

	MIL-100(Fe, Ni) **3** (5%)	3 O	2.04 ± 0.02	6.5 ± 3.2	0.9 % 2314
		3 O	2.09 ± 0.03	10.0 ± 4.7	
		4 C	3.02 ± 0.05	20.4 ± 12.4	
		0.86 Fe	3.30 ± 0.05	5.0 ± 7.5	
		1.14 Fe	3.49 ± 0.07	9.4 ± 11.4	
<u>Fe K edge</u> $S_0^2 = 0.68$ enot= 7127.7 ± 3.0 eV $\Delta k = 3.5 – 11$ Å^{-1} ΔR = 1-3.9 Å	MIL-100(Fe)	3 O	1.95 ± 0.01	0.2 ± 0.7	1.1 % 1597
		3 O	2.07 ± 0.01	0.2 ± 0.6	
		4 C	2.96 ± 0.03	5.8 ± 4.4	
		0.86 Fe	3.32 ± 0.02	1.5 ± 2.7	
		1.14 Fe	3.45 ± 0.03	4.0 ± 3.2	
	MIL-100(Fe, Ni) **3** (5%)	3 O	1.95 ± 0.01	0.5 ± 0.6	1.1 % 1595
		3 O	2.07 ± 0.01	0.5 ± 0.6	
		4 C	2.96 ± 0.03	6.2 ± 4.4	
		0.86 Fe	3.31 ± 0.02	1.9 ± 2.8	
		1.14 Fe	3.44 ± 0.03	4.9 ± 3.5	

Comparison of samples MIL-100(Fe, Ni) **2** and **3**Ni samples in Figure S15 and with the addition of parameters for Ni_5% which are similar to those for the 3%, we clearly see that they are comparable in local order.

In situ IR spectroscopy

a

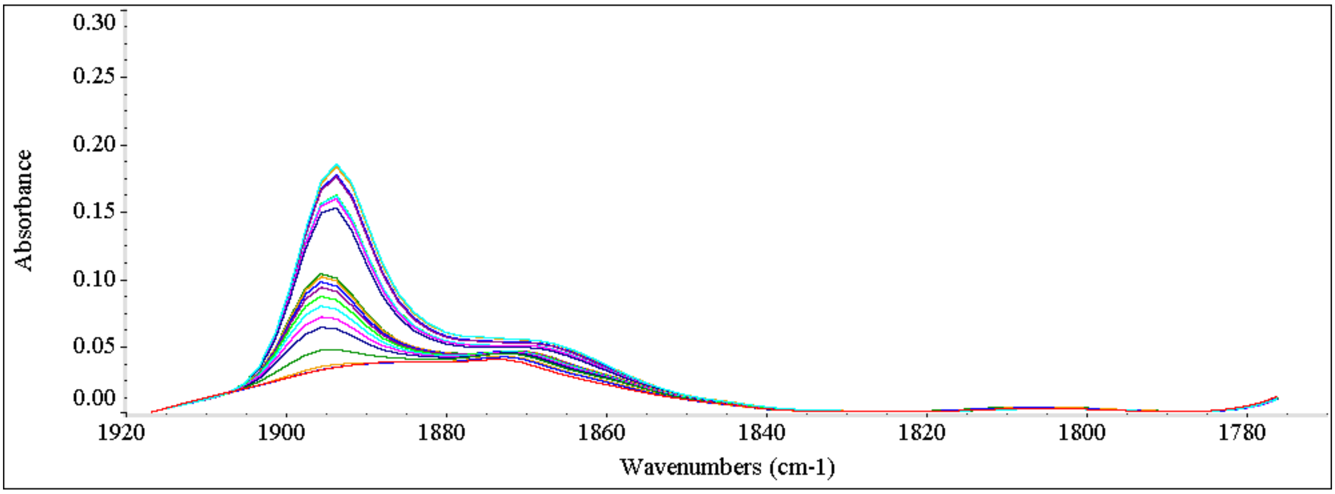

b

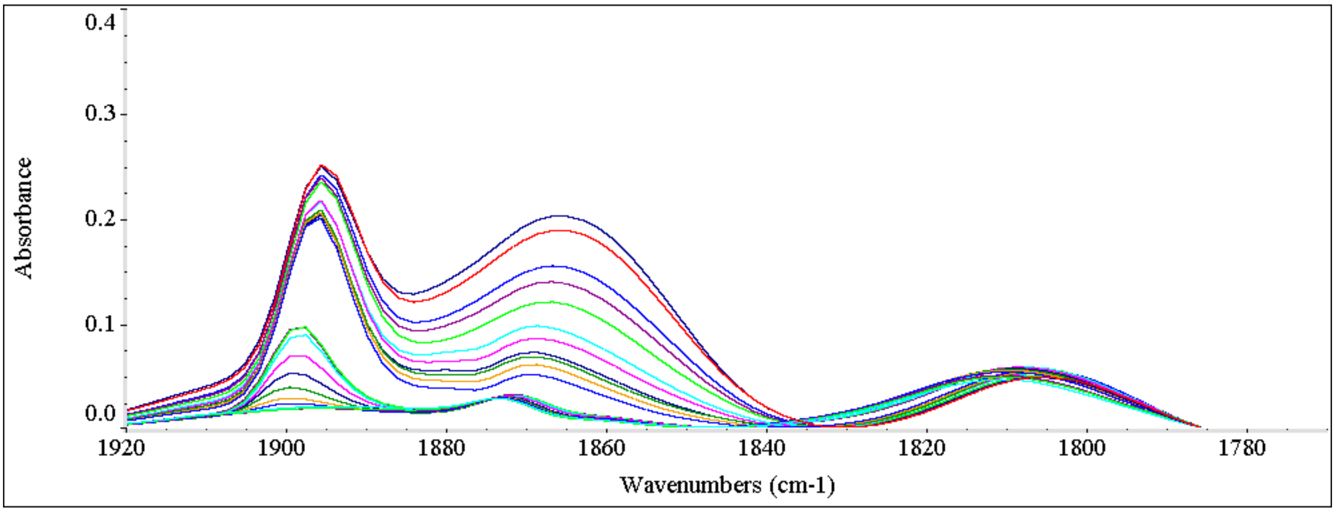

c

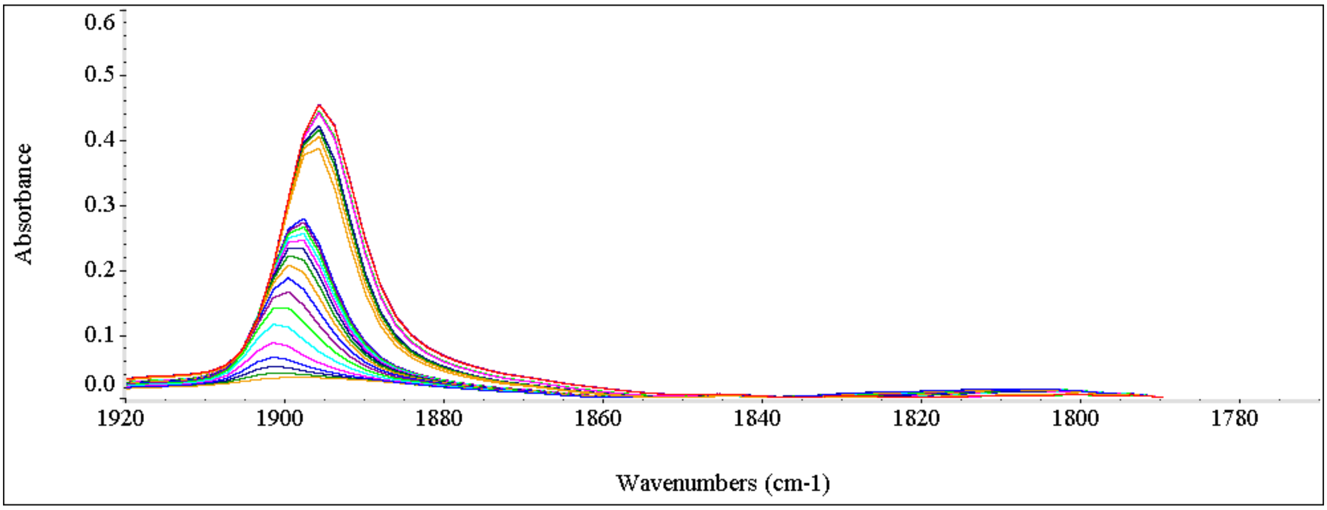

d

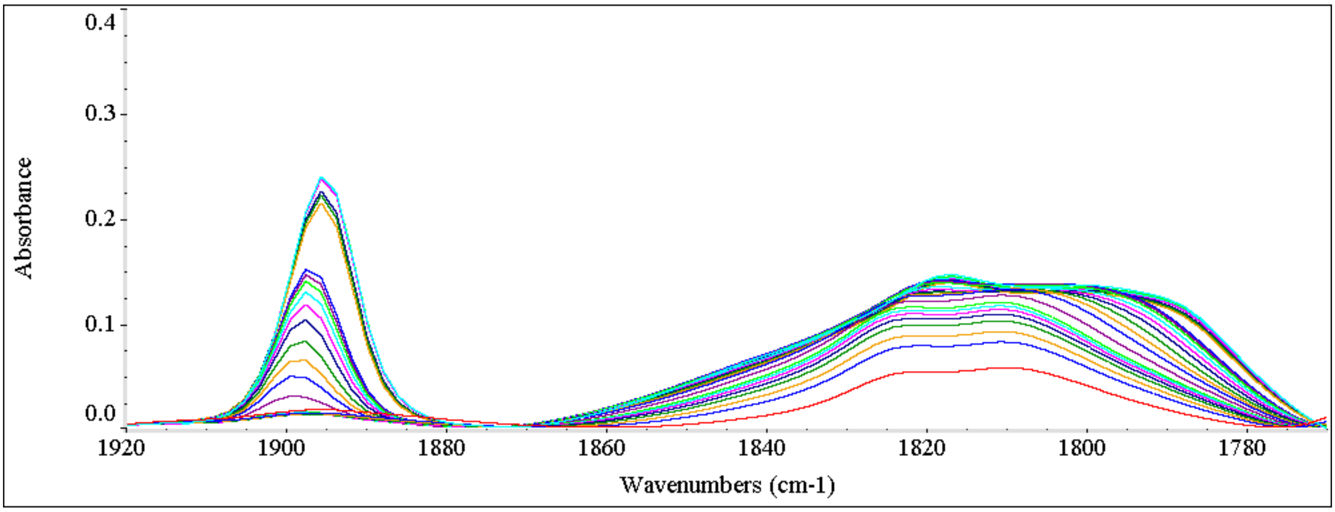

Figure S18. Infrared spectra of MIL-100(Fe, Ni) **3** (a,b) and MIL-100(Fe) (c,d) after introduction of increasing pressures of NO. (a,c) Spectra after activation of the solid at 423 K; (b,d) Spectra after activation of the solid at 503 K.

Catalytic tests.

In a preliminary study, conversion of β-pinene using different amounts of catalyst (0.3, 0.5 and 0.7 mmol % total metal based) was evaluated, concluding that 0.5 mmol % was the optimal amount of catalyst.

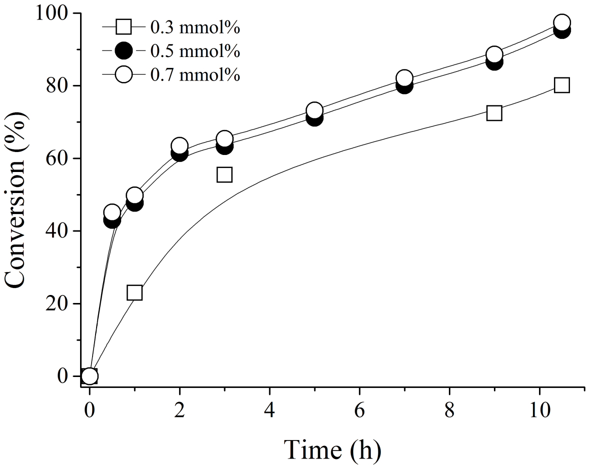

Figure S19. Comparison of the time conversion plot of β-pinene using different amounts of MIL-100(FeNi) **3** catalyst. Reaction conditions: MIL-100(FeNi) **3** catalyst (5, 10 and 15 mg corresponding to 0.3, 0.5 and 0.7 mol% total metal based,), β-pinene (1 mmol) and paraformaldehyde (1 mmol) in MeCN at 80 °C.

Productivity test.

A productivity test using a large excess of β-pinene over mixed-metal MIL-100(FeNi) **3** MOF was performed. For this test, β-pinene (10 mmol) is being converted with only 0.001 mmol of catalyst (Fe+Ni metal based) (1x10^4 Turnover number TON). Under these extreme conditions, full conversions were reached at long reactions times (see Figure 3b). Importantly, a selectivity of 100 % was maintained over the reaction.

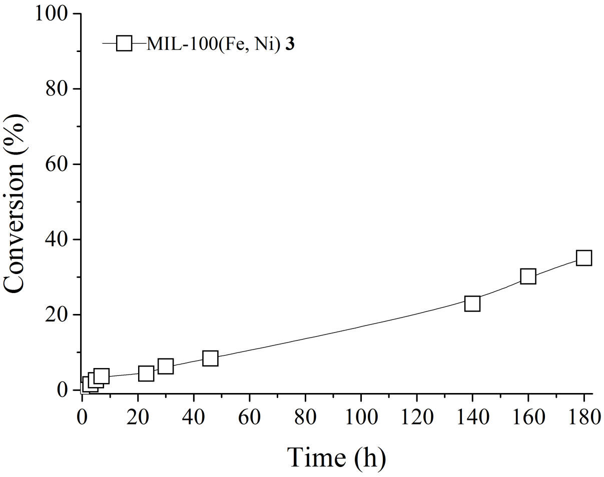

Figure S20. Time conversion plot for the Prins condensation of β-pinene. Reaction conditions: catalyst (3 mg, 0.001 mol% metal), β-pinene (10 mmol) and paraformaldehyde (10 mmol) in MeCN at 80 °C.